ChemPubSoc Europe

DOI: 10.1002/chem.201603214

CHEMISTRY A European Journal Full Paper

Sustainable Chemistry

Impact of Nonthermal Atmospheric Plasma on the Structure of Cellulose: Access to Soluble Branched Glucans

Joakim Delaux,[a, b] Carmen Ortiz Mellet,[c] Christine Canaff,[a] Elodie Fourré,[a] Cédric Gaillard,[d] Abdellatif Barakat,[b] José M. García Fernández,[e] Jean-Michel Tatibouët,[a] and François Jérôme*[a]

Dedicated to Professor James Clark on the occasion of his 65th birthday

Abstract: We have investigated the effect of non-thermal atmospheric plasma (NTAP) on the structure of microcrystalline cellulose. In particular, by means of different characterization methods, we demonstrate that NTAP promotes the partial cleavage of the β-1,4 glycosidic bond of cellulose leading to the release of short-chain cellodextrins that are reassembled in situ, preferentially at the C6 position, to form branched glucans with either a glucosyl or anhydroglucosyl terminal residue. The ramification of cellulosic chain induced by NTAP yields branched glucans that are soluble in DMSO or in water, thus opening a straightforward access to processable glucans from cellulose. Importantly, the absence of solvent and catalyst considerably facilitates downstream processing as compared to (bio)catalytic processes which typically occur in diluted conditions.

Introduction

Cellulose is a natural linear polymer of β-D-glucopyranose in which the monosaccharide units are covalently linked through β-1,4 glycosidic linkages.[1] Cellulose is naturally produced in large scale by living organisms and has long been used for the production of fibers or paper. Its polysaccharide structure also confers promising properties for the synthesis of industrially relevant materials such as surfactants, glues, thickening agents or viscosity modifiers, to mention but a few. Nature has however designed cellulose as a robust polymer in which the polysaccharide chains are stacked together by the interplay of an extensive hydrogen-bond network,[2] van der Waals interactions[3] and electronic effects.[4] Altogether, this makes chemical processing of cellulose for technological applications rather complex. To produce soluble and thus processable materials, cellulose is often derivatized.[5] For instance, hydroxyethyl- and carboxymethylcellulose or cellulose acetate, which are manufactured in large scale. These derivatization processes however produce a large amount of salts and sometimes require hazardous or corrosive chemicals such as chloroacetic acid, acetic anhydride, ethylene oxide, epichlorohydrin, etc. Another strategy consists in the controlled depolymerization of cellulose to cellodextrins, which are processable short cellulosic chains (degree of polymerization, DP < 10). In this case, biocatalysts are often preferred over acid catalysts since they allow a better control of the reaction selectivity.[6] Despite pilot productions, biocatalytic production of cellodextrins remains cost-prohibitive for industrial use mostly due to the price of enzymes, their low stability and costly downstream processing (high dilution ratio).

Recently, Schüth, Rinaldi and Blair reported the mechanocatalytic depolymerization of cellulose to water-soluble low-molecular-weight oligosaccharides (DP = 5–7).[7] The concept of this work is based on a synergistic effect between an acid catalyst (often strong mineral acid such a H_2SO_4 or HCl) and mechanical forces. Mechanical forces not only induce intimate contact between cellulose and the acid catalyst but also facilitate the conformational change of the pyranic ring and thus the cleavage of the β-1,4 glycosidic bond.[4a] At the same period, our group reported pioneer investigations on the partial depolymerization of cellulose by non-thermal atmospheric plasma (NTAP).[8] These preliminary studies showed that using NTAP it was possible to partly and selectively cleave the β-1,4

[a] J. Delaux, C. Canaff, Dr. E. Fourré, Dr. J.-M. Tatibouët, Dr. F. Jérôme
Institut de Chimie des Milieux et Matériaux de Poitiers
CNRS/Université de Poitiers, ENSIP, 1 rue Marcel Doré
Bat 1, TSA 41105, 86073 Poitiers Cedex 9 (France)
E-mail: francois.jerome@univ-poitiers.fr

[b] J. Delaux, Dr. A. Barakat
UMR IATE, CIRAD, Montpellier SupAgro, INRA
Université de Montpelier, 34060, Montpellier (France)

[c] Prof. C. Ortiz Mellet
Dpto. Química Orgánica, Faculty of Chemistry
University of Sevilla, c/Profesor García González 1, 41012 Sevilla (Spain)

[d] Dr. C. Gaillard
INRA, UR 1268 Biopolymers Interaction Assemblies (BIA)
Centre Angers-Nantes, Rue de la Géraudière, 44000 Nantes (France)

[e] Prof. J. M. García Fernández
Instituto de Investigaciones Químicas (IIQ)
CSIC - University of Sevilla, Avda. Americo Vespucio 49
41092 Sevilla (Spain)

Supporting information for this article is available on the WWW under http://dx.doi.org/10.1002/chem.201603214.

glycosidic bond of cellulose without assistance from catalyst or solvent.

To date, the exact mechanism at play during NTAP-promoted depolymerization of cellulose is unknown. Because NTAP generates radicals in the gas phase we can reasonably hypothesize that these radicals react with the surface of cellulose to form sugar radicals (observed by electron spin resonance [ESR]) ultimately leading to bond cleavage.[9,10] Given the highest stability of anomeric carbon radicals as compared with radicals at other positions of the monosaccharide units, the glycosidic linkages are preferentially broken.[11] The impact of NTAP on the macrostructure of cellulose (ramification, oxidation, depolymerization, etc.) remains however unsolved.

The NTAP technology is already implemented at an industrial level for the treatment of powders, liquids or gases. For instance, NTAP is used in large scale for the treatment of cellulose fibers, wood and textile, particularly to change their surface hydrophilicity, mechanical strength, surface erosion, surface roughness, etc.[10] Yet, to date NTAP has never been deployed for the production of processable polysaccharides from cellulose.

Following our two previous reports in the field,[8] we have now conducted a detailed investigation on the (macro)molecular structure of the poly- and oligosaccharides recovered after NTAP treatment of cellulose, thus providing insights on the reaction mechanism. In particular, we show here that NTAP does not only induce depolymerization reactions of cellulose, with formation of cellodextrins and 1,6-anhydro-cellodextrins, but also promotes random repolymerization reactions (also known as reversion reaction) leading to branched glucans. Whereas cellodextrins are linear oligosaccharides exclusively made of β-1,4 glycosidic linkages, the branched glucans arising from reversion reactions are poly- or oligosaccharides in which the glucosyl units are connected through different types of glycosidic linkage (α/β 1,4, 1,3, 1,6, 1,2). This is an important result in view of improving processability, since branching drastically improves the solubility of glucans in water and in organic solvents.

Results and Discussion

NTAP treatment and characterization of glucans

In order to facilitate the characterization of cellulose obtained after NTAP, highly purified microcrystalline cellulose (MCC) PH AVICEL 200 was selected. This MCC grade has been well characterized previously. It has a content of glucose higher than 99%, a degree of polymerization (DP) of 200, a water content of 5 wt% and a particle size of 150–250 μm. The crystallinity index (CrI) of MCC is 80%. For the sake of clarity, it is abbreviated to MCC-80 in the following discussion, where 80 stands for the CrI. As the structural order of cellulose affects the efficiency of NTAP in a sensitive way, MCC samples with different crystallinity indexes were also prepared. To this end, MCC was vibro-ball milled for different periods of time to produce samples of MCC with a crystallinity index of 50, 20, 30, 10 and <10% named here MCC-50, MCC-20, MCC-30, MCC-10 and MCC<10, respectively. The crystallinity index was determined by X-ray diffraction (XRD) analysis. Please note that after the vibro-ball milling, the degree of polymerization of cellulose (DP) was slightly decreased (Figure 1 at $t=0$). Particle sizes are between 80 and 50 μm for vibro-ball-milled cellulose.

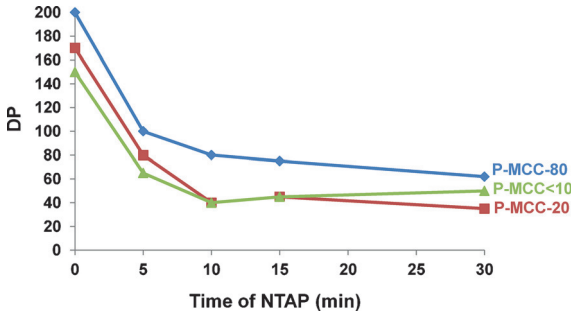

Figure 1. Plot of the DP (±30) of MCC as a function of the NTAP treatment time.

In a typical procedure, 0.3 g of MCC-*X* (*X*<10 or *X*=10–80) was placed between two parallel square-electrodes (copper) of 25 cm^2 isolated from each other by a dielectric material (commonly named dielectric barrier discharge (DBD) reactor; Figure S1 in the Supporting Information). To maintain an optimal plasma discharge, the gap between both electrodes was fixed to 4 mm. To create the plasma discharge, a bipolar pulse signal was used at a maximum voltage of 10 kV at 2.2 kHz frequency (i.e., 15 W). All reactions were conducted under air at a flow rate of 100 mL min^{-1}. The NTAP-treated MCC were abbreviated P-MCC-*X* (with *X*=10–80) in the following discussion.

Samples were taken from the DBD reactor at different treatment times and the DP was roughly assessed by viscosity analyses by using the NF G 06-037 norm (Supporting Information). The plot of the DP of MCC as a function of the NTAP treatment time is provided in Figure 1. Interestingly, whatever the crystallinity index of the starting MCC, a rapid decrease in the DP was observed during the first 10 min of NTAP and then a plateau was reached (see later for more information on this phenomenon). A similar phenomenon was also observed using other grades of cellulose such as α-cellulose and Whatman filter paper for instance (Figure S2).

Although NTAP cannot totally depolymerize the MCC samples, we noticed that the NTAP treatment led to a drastic change in the solubility of MCC. The Figure 2 shows the solubility of P-MCC in water or dimethylsulfoxide (DMSO) as a function of the CrI of the starting MCC. Typically, 50 mg of P-MCC sample was immersed in 10 mL of DMSO or water and stirred at 80 °C for 300 min. The percentage of solubilization given in Figure 2 was determined by weighting the amount of insoluble P-MCC after filtration and drying.

Whereas all MCC-*X* (*X*=<10 to 80) samples were sparingly soluble in DMSO or water, their solubility was markedly enhanced after the NTAP treatment (P-MCC). As a general trend, the lower the crystallinity index of cellulose, the higher the solubility of the obtained P-MCC product. For instance, P-MCC<

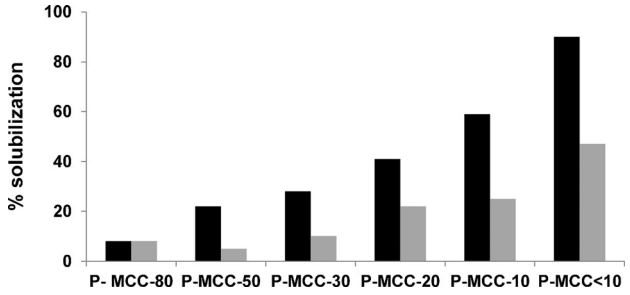

Figure 2. Solubilization of P-MCC in DMSO (black columns) and water (gray columns) as a function of the crystallinity of the starting MCC.

10 was nearly fully soluble in DMSO and partly in water (50 wt%) after only 15 min of exposure to NTAP, indicating that the NTAP treatment can convert cellulose to processable polysaccharides—an important aspect with respect to cellulose processing.

The difference of solubility between MCC and P-MCC suggests that NTAP has led to a drastic change in the (macro)molecular structure of MCC. To obtain a deeper insight on this phenomenon, the (macro)molecular structure of P-MCC was investigated by means of different analytical methods. First, the chemical transformations promoted by NTAP treatment of MCC-80, MCC < 10 and P-MCC < 10 particles were analyzed by X-ray photoelectron spectrometry (XPS) which provides information on the chemical composition of the surface of a material in a layer of up to 10 nm. Results are summarized in Table 1. Control experiments confirmed that the surface chemical composition of MCC < 10 was similar to that of MCC-80, indicating that the vibro-ball milling only affected the structural order of MCC-80. Conversely, the surface chemical composition of P-MCC < 10 was significantly different as compared with that of MCC < 10 (Figure S3). Particularly the proportion of C–O bonds markedly decreased to 49.8% (vs. 73.3% for MCC < 10) after exposure to NTAP, which was accompanied by the formation of –O–C=O groups, indicating that oxidation occurred. The detection of a very weak band at 1750 cm^{-1} in the corresponding FT/IR spectrum, consistent with the presence of –C=O groups, confirmed this observation.

To determine whether or not NTAP-promoted oxidation is propagated to deeper regions in the cellulose material, a P-MCC < 10 sample was next analyzed by solid state ^{13}C CP/MAS NMR spectroscopy (Figure S4). No peak ascribable to carbonyl groups was detected, suggesting that oxidation remained restricted to the surface of particles only and did not occur to a significant extent in the bulk.

Table 1. Effect of NTAP on the chemical composition of the surface of MCC samples (C1s).[a]

MCC sample	C–O [%]	O–C=O [%]	O–C–O [%]
MCC-80	69.3	5.1	25.6
MCC < 10	73.3	1.8	24.9
P-MCC < 10	49.8	18.0	30.9

[a] Adventitious carbon-based contaminant, with the binding energy of 284.8 eV was used as the reference for calibration.

Consistent with the ^{13}C CP/MAS NMR spectroscopy, no evidence for the formation of –C=O and –CHO bands was observed by Raman spectroscopy (1700–1750 cm^{-1}), further confirming that oxidation occurs to a very low extent. The evolution of the Raman spectra of the initial MCC-80 was followed as a function of the vibro-ball milling time and subsequent NTAP treatment (Figure S5). The characteristics bands of MCC are in the window 300–1500 cm^{-1} with typical bands at 1335 cm^{-1} (–CH_2–, –OH vibrations), 1120 and 1096 cm^{-1} (symmetric and asymmetric stretching vibrations of the glycosidic C–O–C bond, respectively), 379 cm^{-1} (C–C–C bending vibrations of glucosyl rings, typical for crystalline cellulose).[12] As compared to MCC-80, the Raman spectra of MCC-20, MCC-10 and MCC < 10 clearly indicate an increase of the typical vibrations of amorphous cellulose located at 1260 and 1460 cm^{-1} (H–C–H/H–O–C bending) which is fully consistent with previous Raman spectroscopy based results on ball-milling (Figure S5). Treatment of MCC-80 by NTAP led to slight enhancements of the vibrations ascribed to amorphous cellulose, suggesting that chemical transformations, different from the predominant oxidation processes occurring at the particle surface, take place in the bulk leading to alterations in the macromolecular structure of cellulose (Figure S5). Monitoring of the diagnostic Raman bands of P-MCC samples at 349 cm^{-1} (C–C–C vibrations of the glucosyl rings, typical for amorphous cellulose), 520 cm^{-1} (C–C–C vibrations of the glucosyl ring and the glycosidic bond), 1120 cm^{-1} (symmetric vibrations of the glycosidic bond) and 1379 cm^{-1} (–CH_2– bending and skeletal vibrations), the intensities of which are only slightly modified after milling but markedly increased after NTAP treatment, strongly support this hypothesis.

Principal component analysis (PCA) is a regression method and was used in this work to obtain a fine analysis of the Raman data of MCC and P-MCC samples. Particularly, it allows detection of the crystalline and amorphous nature of the cellulosic samples as well as chemical backbone modifications (Figure 3). The loading line plots of the two main components PC1 and PC2 showed that Raman spectral differences appeared after the ball milling and NTAP step (Figure S6). Crystallinity can be assessed from the PC1 and PC2 positive bands at 377–379 cm^{-1}. Inversely, the amorphous feature is indicated by the PC1 negative bands at 1263 and 1460 cm^{-1}. Then, it can be confirmed from Figure 3 that whatever the initial CrI of MCC, P-MCC samples were always more negative than MCC either along with the PC1 or PC2 loading line plots. These results suggest that NTAP enhanced a further reduction in the crystallinity of MCC in line with a change in the chemical structure of the cellulosic backbone. One can also notice that the lower the CrI of the starting MCC, the more pronounced the structure modification induced by NTAP. The PC loading lines exhibit also characteristic bands corresponding to the chemical structure of the cellulosic skeleton. PC1 and PC2 positive bands at 434–435 cm^{-1} (C–C–C and C–C–O ring deformation) mark the integrity of the glucose rings as well as the PC2 positive band at 1120 cm^{-1} (symmetric C–O–C glycosidic bond).

The ESI and MALDI-TOF mass spectra of the water-soluble fraction of P-MCC samples revealed two series of monocation-

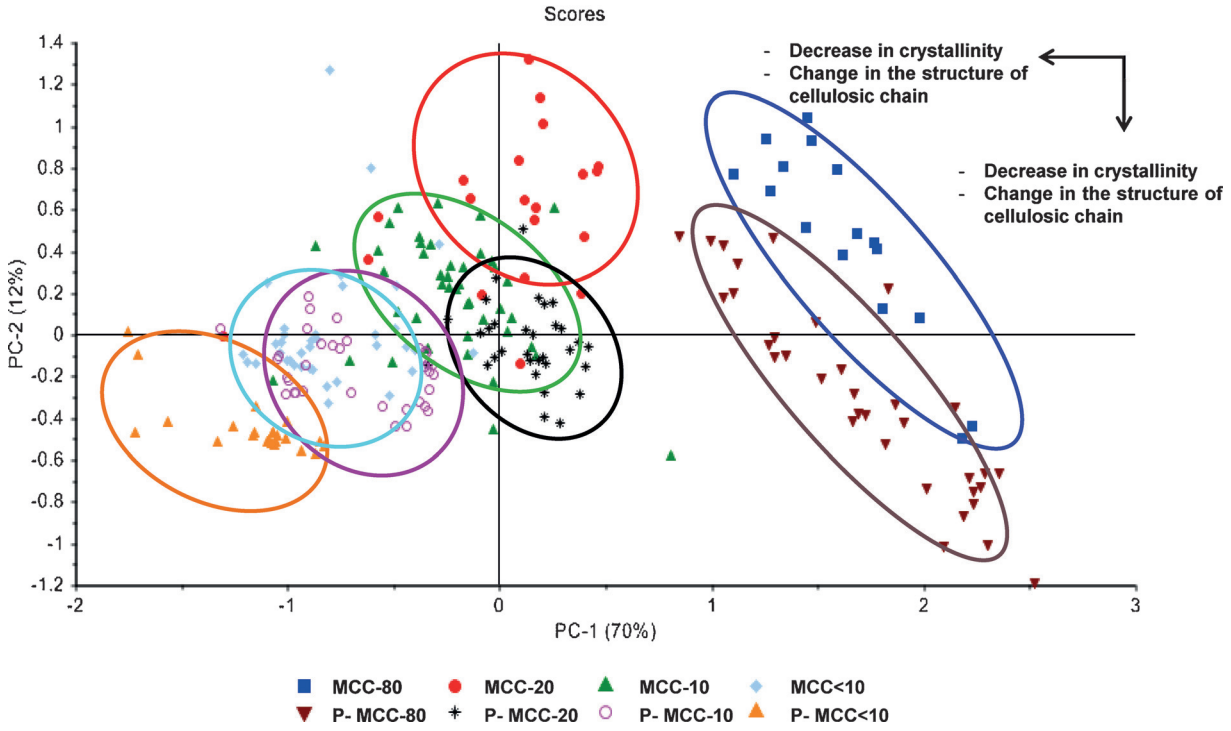

Figure 3. Principal component analysis of the Raman spectral data of MCC and P-MCC.

ized pseudomolecular peaks with sequential *m/z* increments of 162 units that correspond to an additional monosaccharide residue (Figure 4). One of these series stems from the expected reducing oligosaccharides arising from cellulose partial hydrolysis. The other series, with peaks that differ in −18 mass units from the previous one, probably accounts for 1,6-anhydrooligosaccharides. Formation of, 1,6-anhydro-cellooligosaccharides has been previously observed during acidic or thermal (pyrolysis) depolymerization of cellulose and seems to be also a significant reaction pathway during NTAP activation.[13]

Raman or MS data do not provide direct information on the overall architecture (linear or branched) of the product resulting from NTAP treatment of cellulose. To assess the effect of NTAP on the chemical structure of the cellulosic chain, the branching pattern of the P-MCC < 10 sample was next analyzed by gas chromatography coupled to mass spectrometry (GC-MS) after methylation analysis (ESI). To this end, an aliquot of the crude product in dimethylsulfoxide/water (5:1) was first subjected to extensive methylation by treatment with methyl iodide and sodium methoxide (twice) to etherify the free hydroxyl groups in the oligosaccharides.[14] The glycosidic bonds in the permethylated species were next hydrolyzed by treatment with trifluoroacetic acid (TFA) at 120 °C, thus affording the reducing monosaccharide components. Subsequent reduction with sodium borodeuteride and acetylation with acetic anhydride/TFA affords the corresponding alditols labeled with deuterium at C-1, methylated at non-glycosylated positions and bearing acetyl groups at positions that were originally glycosylated in the starting oligosaccharides.[15] Most of the products obtained through this protocol were glucitol derivatives that could be unequivocally assigned from the corresponding

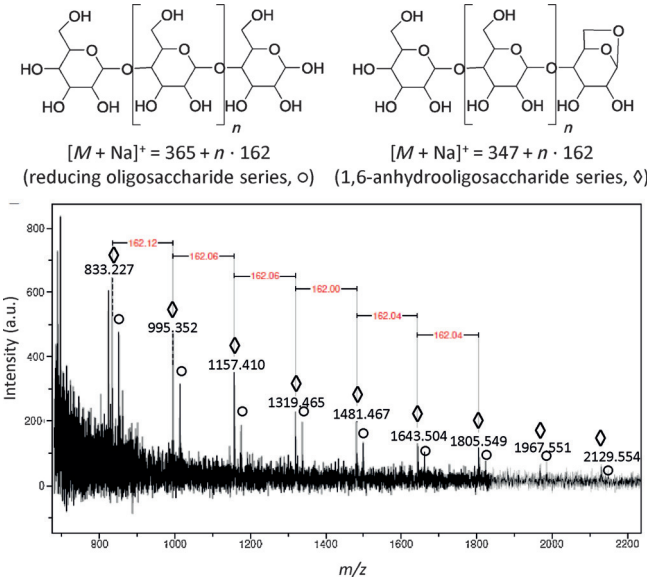

Figure 4. MALDI-TOF mass spectra of the P-MCC < 10 sample showing the two series of pseudo-molecular peaks corresponding to 1,6-anhydro (◊) and reducing oligosaccharides (○).

MS fragmentation patterns, after GC separation, by comparison with authentic standards.[16] The results are summarized in Table 2.

Comparison of the data obtained for MCC < 10 and P-MCC < 10 shows that the amount of O-4 glycosylated glucopyranosyl units decreases from 95.6 to 78.8% after NTAP treatment. Concomitantly, the proportion of non-reducing terminal monosaccharide units increased from 1.4 to 4.6%, which is in agree-

Table 2. Relative proportions [%] of non-reducing terminal, O-4, di-O-4,6-, di-O-3,4- and di-O-2,4-substituted glucopyranosyl residues in MCC < 10 and in the corresponding product obtained by NTAP treatment (P-MCC < 10).[a]

MCC sample	Non-reducing terminal	O4-O1	O4-(O1,O6)	O4-(O1,O3)	O4-(O1,O2)
MCC < 10	1.4	95.6	3.0	0	0
P-MCC < 10	4.6	78.8	12.0	2.6	1.9

[a] Errors are estimated to be about 20%.

ment with a decrease in the average DP of the chains induced by NTAP. Most interestingly, up to 16.5% of the 4-O-linked glucosyl residues are branched at a second hydroxyl position, preferentially at O-6. From Table 2, it appears that at least 1 in 8 glucose units in the cellulose chain of P-MCC < 10 were branched at the primary position and 1 in 6 was branched at either O-2, O-3 or O-6 (Scheme 1). One should note that no fragments monoglycosylated at a position other than O-4 were detected, meaning that the β-1,4 backbone of cellulose was essentially preserved in the P-CCM < 10 oligomers. Altogether, these results suggest that NTAP treatment partly breaks the β-1,4 glycosidic bond affording shorter cellulosic chains that are then recombined through reversion reaction with dominant 1,6 linkage to produce soluble glucans. Formation of branched glucans is also supported by XPS analyses which revealed an increase in the amount of O–C–O bond after NTAP treatment (Table 1).

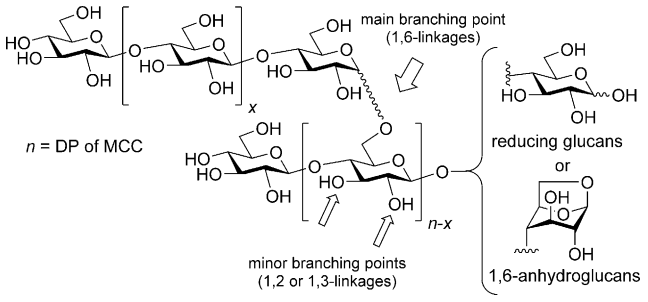

Scheme 1. Proposed chemical structure of glucans produced by NTAP.

NTAP is commonly used for the treatment of surfaces. However, one can point out from Figure 2 that the effect of NTAP on the solubilization of MCC is closely depending on the CrI of the starting MCC. In other words it indicates that active species (presumably radicals) formed on the surface of cellulose particles can diffuse more or less deeply within the bulk (as a function of the CrI of the starting MCC) where they lead to the formation of branched glucans. To further assess to which extent the reorganization of the MCC structure has occurred in the bulk, the reactivity of the glycosidic bonds after NTAP was probed by using acid-catalyzed hydrolysis as a model reaction. Branched glucans are more readily hydrolyzed to glucose under diluted acid conditions than MCC due to their greater solubility in water and also due to the presence of glycosidic bonds with a higher sensitivity to hydrolysis than the β-1,4 linkage found in cellulose. Consequently, the yield of recovered glucose would provide an indication of the extent of the structural reorganization of the MCC to glucan chains in bulk. Typically, P-MCC samples (250 mg) were heated in 10 mL of water at 150 °C under microwave irradiation (300 W) for 1 h in the presence of 9 wt% of H_2SO_4. The production of glucose was monitored by HPLC using an NH_2-column and a RID detector (Supporting Information). The results are presented in Table 3 and Figure 5.

Table 3. Impact of the NTAP treatment on the acid-catalyzed hydrolysis of MCC-80.

MCC grade	Yield of glucose [%]
MCC-80	5
P-MCC-80	15
recovered P-MCC-80[a]	5
PP-MCC-80	12

[a] After the first catalytic hydrolysis.

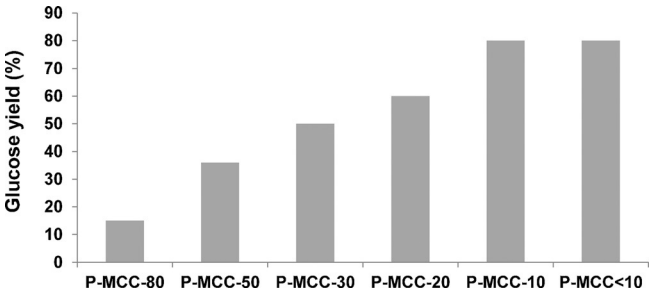

Figure 5. Acid-catalyzed hydrolysis of P-MCC. NTAP treatment $t = 15$ min for each sample.

In agreement with previous reports, when MCC-80 was treated under these conditions free glucose was obtained with a maximum yield of 5%, which is consistent with the high recalcitrance of MCC-80 towards hydrolysis (Table 3). Starting from P-MCC-80, the yield of glucose was enhanced from 5 to 15% showing the effect of NTAP on the sensitivity of the glycosidic bonds (Table 3). The unreacted P-MCC-80 recovered by filtration at the end of the catalytic hydrolysis process was found to be highly recalcitrant to hydrolysis. When unreacted P-MCC-80 was treated again by NTAP (named PP-MCC-80 in Table 3) and re-engaged in the catalytic hydrolysis process, 12% yield of glucose was obtained, suggesting that in this case, that NTAP has mostly affected by the surface of MCC-80.

As illustrated in Figure 5, the maximum yield of glucose markedly increased when the CrI of the starting MCC was lowered prior the NTAP treatment, suggesting a deeper reorganization of the cellulosic chain in the bulk. For instance, catalytic hydrolysis of P-MCC-80, P-MCC-50, P-MCC-30, P-MCC-20 and P-MCC-10 affords glucose with a yield of 15, 35, 50, 60 and 80%, respectively. Without any NTAP treatment, yields of glucose remained within the range 5–10%, which further supports the

impact of NTAP on the reactivity of recovered glucans. Conversely to what is generally observed with MCC, the catalytic hydrolysis of P-MCC samples was highly selective. For instance, in the case of P-MCC-10, 80% yield of glucose was obtained at a conversion of 83% which highlights the drastic change in the reactivity of MCC in water after NTAP.

At this stage, two hypotheses can be drawn to explain the deep reorganization of MCC with low CrI promoted by NTAP. One may indeed suspect that the diffusion rate of active species from the surface to the bulk is impacted by: 1) the cohesive hydrogen-bond network of MCC, and/or 2) the water content of MCC. Reducing the structural order of MCC indeed concomitantly increases its hygroscopic properties (Figure S7). For instance, MCC-80 has a water content of 5 wt% while MCC-10 has a water content of 11 wt%. To obtain more information on the role of water, MCC-10 was freeze-dried to reduce its water content to 5 wt% (similar to MCC-80). After NTAP treatment and catalytic hydrolysis, the yield of glucose was decreased to 45% (vs. 80% without freeze-drying) suggesting that water trapped in the cellulose backbone does play a major role.

To further support the role of water, the DBD reactor was coupled to a mass spectrometer to check the water content in the gas phase (Figure 6). Analysis was conducted here on α-cellulose but similar results were observed with MCC samples. α-Cellulose has a water content of 7 wt%. During the first 10 min of NTAP, there is a clear release of water in the gas phase which was ascribed to the drying of the sample. After 10 min of exposure to NTAP, TDA/TGA analyses revealed that the water content of cellulose decreases from 7 to 2 wt%. During this period ("rich water phase"), depolymerization of α-cellulose is the dominant reaction (Figure 6). Then, the water content decreased and reached a plateau when the depolymerization reaction ceased. During this "water-poor phase", an equilibrium was reached that probably involves competitive depolymerization/repolymerization reactions as well as 1,6-anhydrization of reducing units, which is further supported by our previous report on the polymerization of mono- and disaccharide induced by NTAP.[17]

Tentative mechanism

The exact mechanism governing NTAP-promoted transformations of MCC is difficult to elucidate given the lack of appropriate techniques for real-time in situ monitoring of the structural changes occurring in the bulk. Nevertheless, from the current body of experimental evidence, a general picture can be advanced, although we are fully conscious that further investigations are still needed (Figure 7). Under air, it is known that a complex cocktail of excited species, and notably radicals, are formed in the DBD reactor. These radicals react with the surface of MCC to produce glycosyl radicals that have been previously characterized by ESR spectroscopy.[9,10] It is interesting to speculate that these radicals may readily react with water contained in the MCC structure to produce $OH^{\bullet}$ radicals, which subsequently induce glycosidic bond cleavage by propagation reaction from the surface to the bulk. The preferential cleavage of the glycosidic bond by hydroxyl radicals is further supported by previous works.[9–11] As long as water is present in the MCC backbone, depolymerization reactions are dominant. During NTAP, MCC is however concomitantly partly dried as suggested by TDA/TGA and on-line mass spectrometry analyses (Figure 6). The decrease in water content of MCC activates (intermolecular) repolymerization and (intramolecular) 1,6-anhydrization reactions that then become dominant. The primary hydroxyl group is the most accessible one and thus acts as the preferred acceptor for the former reactions, leading to the dominant formation of O-6 branched glucans. Attempts to enhance depolymerization reactions by adding water in the NTAP gas phase failed, suggesting that only water included in the structure of MCC is involved in the propagation stage.

Oxidation of MCC (formation of –COO– groups) occurs to a low extent and only at the surface of the MCC particles, which is in direct contact with the NTAP gas. This result suggests that excited species formed in the NTAP gas do not diffuse within the bulk of MCC but initiate the formation of hydroxyl radicals, which might be the real species responsible for the depolymerization/repolymerization reactions of cellulosic chains.

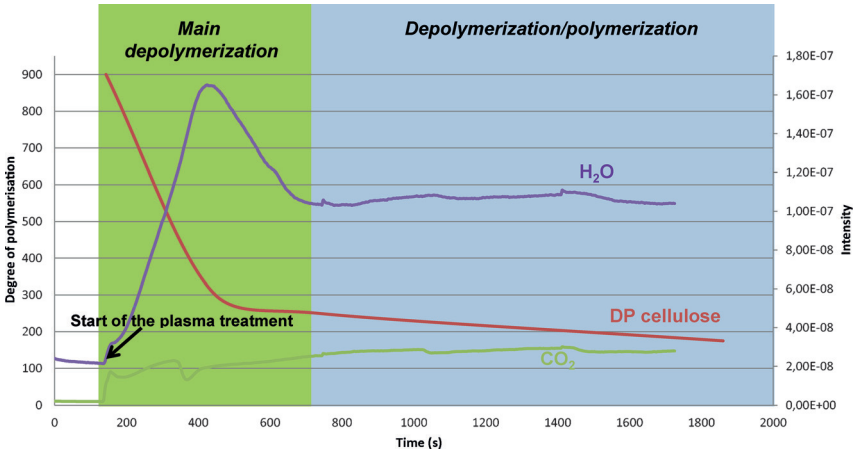

Figure 6. Monitoring of water in the gas phase of the DBD reactor by coupling with MS.

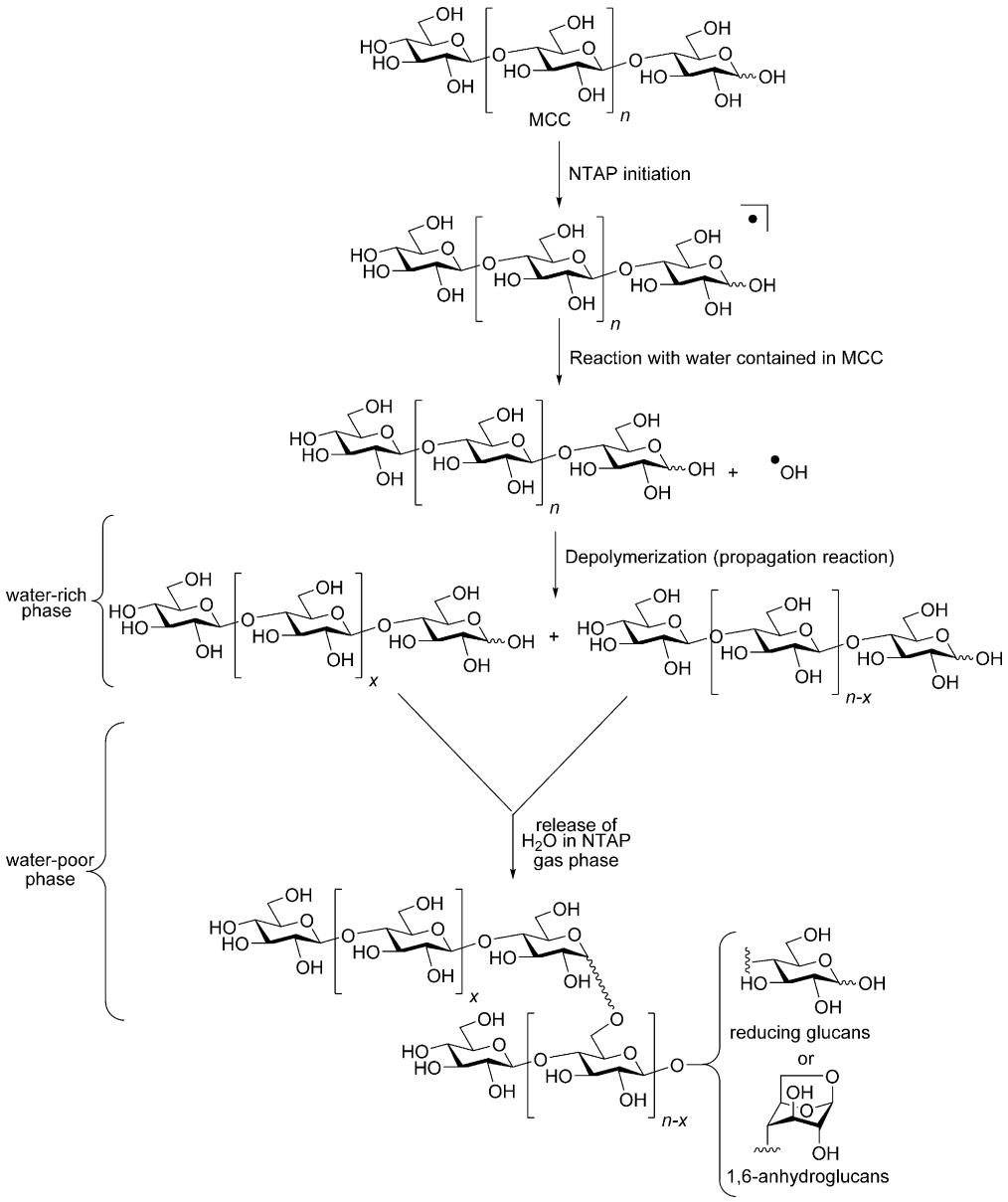

Figure 7. tentative mechanism to explain the modification of the cellulosic chain structure induced by NTAP.

Energy consumption

Although NTAP can provide processable polysaccharides from MCC-*X* (*X* ranging between <10 and 80) without any solvent or catalyst (no downstream processing), the electricity cost remains an important cost driver. Despite the fact that the DBD reactor used in this study is clearly not the optimal one for industrial transposition, calculation of the energy requirement provides a rough idea on the viability of NTAP for glucan productions from MCC. The price of energy being cheaper in the US than in the EU, the former has been used as a reference in this section (0.07 $ per kWh).

The energy requirement measured for the NTAP treatment (0.3 g of MCC-*X*, 15 min) is 12.5 kWh per kg of MCC-*X* corresponding to an electricity cost of 0.88 $. In the configuration of our DBD reactor, the amount of treated MCC-*X* can be increased to 0.8 g without affecting the NTAP efficiency, thus reducing the electricity cost to 0.33 $.

The solubility of P-MCC samples closely depends on the CrI of the starting MCC. Hence, the total energy requirement (E_{total}) to obtain soluble glucans from MCC should be written:

$$E_{total} = E_{milling} + 0.33$$

where $E_{milling}$ and 0.33 represent the electricity cost associated to the vibro-ball milling technology and the NTAP treatment, respectively. Figure 8 presents the plot of the E_{total} as a function of the solubility of P-MCC-*X* in DMSO.

There exists a quasi-linear relationship between E_{total} and the solubility of P-MCC-*X* in DMSO. The highest solubility (90%) was obtained after 15 min of NTAP treatment of MCC <10. The

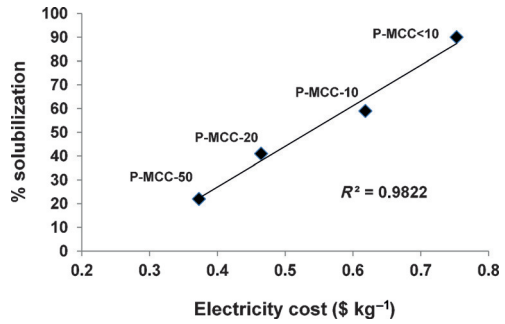

Figure 8. Solubility of P-MCC-*X* as a function of the electricity cost.

energy required by the milling to obtain MCC < 10 is 6.04 kWh kg^{-1}, that is, an electricity cost of 0.42 $. The E_{total} required to obtain 90% solubility of cellulose in DMSO is thus 0.75 $. The current price of the cellulosic pulp is about 0.8 $ kg^{-1} suggesting that processable glucans with a price of at least 1.55 $ kg^{-1} could be obtained, which is in a promising range for application as a biobased material considering the current price of cosmetic grade hydroxyethylcellulose (≈5 $ kg^{-1}), carboxymethylcellulose (≈2–4 $ kg^{-1}) or glucans (>5–10 $ kg^{-1}).

One should note that the scale-up of these technologies will definitely contribute to significantly decrease the electricity cost as previously demonstrated by Rinaldi, Schüth and Blair's groups and thus lower the price of processable P-MCC-*X*.[7]

Conclusions

By means of different characterization methods, we show that NTAP is capable of promoting the partial cleavage of the β-1,4 glycosidic bond of cellulose leading to the release of short chain cellodextrins that are further reassembled in situ, preferentially at the C6 position, leading to branched glucans with either a glucosyl or anhydroglucosyl terminal residue. The extent to which the cellulosic chain is reorganized depends on the CrI of cellulose. Although deeper investigations are still needed to fully disclose the reaction mechanism at play during the NTAP treatment of cellulose, the first collected results suggest that the highest amount of water contained in cellulose with a low CrI is partly responsible for this phenomenon. Importantly, the ramification of cellulosic chain (on average 1 ramification each 6 glucosyl units) after NTAP leads to the formation of glucans that are soluble in DMSO and even partly in water, opening a straightforward route to processable polysaccharides from cellulose. The reorganization of the cellulosic chains induced by NTAP occurs within only 10 min and without assistance from any solvent or catalyst, thus considerably facilitating downstream processing (no purification is required) as compared to conventional (bio)catalytic routes which occur typically under diluted conditions. In addition, NTAP does not damage the glucosyl unit and glucans are recovered as a white solid at the end of the treatment.

We believe that NTAP has a real potential breakthrough not only for cellulose processing, but also to potentially access to a wide range of industrially relevant glucans directly from cellulose as a nonedible raw material. We would like to draw the attention of the reader to the fact that the energy consumption of NTAP is in line with material applications but, to date, not for the production of low value chemicals such as glucose, furanic derivatives, etc. The scale-up of this process is now under progress in our group and should demonstrate the profitability of this technology for accessing cost-competitive processable polysaccharides from cellulose.

Acknowledgements

Authors are grateful to the CNRS and the French Ministry of research for the financial support. J.D. also thanks the CNRS and INRA for his PhD grant. M.C.O. and J.M.G.F. thank the MINECO (contract numbers SAF2013-44021-R and CTQ2015-64425-C2-1-R), the Junta de Andalucía (contract number FQM2012-1467), and the European Regional Development Funds (FEDER and FSE) for financial support. The CITIUS (University of Seville) and the analytical services of IIQ are also thanked for technical support.

Keywords: biomass · cellulose · glucans · non-thermal atmospheric plasma · polysaccharides

[1] For selected reviews on cellulose see: a) D. Klemm, B. Heublein, h.-P. Fink, A. Bohn, *Angew. Chem. Int. Ed.* **2005**, *44*, 3358–3393; *Angew. Chem.* **2005**, *117*, 3422–3458; b) D. Klemm, F. Kramer, S. Moritz, T. Lindström, M. Ankerfors, D. Gray, A. Dorris, *Angew. Chem. Int. Ed.* **2011**, *50*, 5438–5466; *Angew. Chem.* **2011**, *123*, 5550–5580; c) I. Siró, D. Plackett, *Cellulose* **2010**, *17*, 459–494; e) R. J. Moon, A. Martini, J. Nairn, J. Simonsen, J. Youngblood, *Chem. Soc. Rev.* **2011**, *40*, 3941–3994.

[2] a) M. Poletto, V. Pistor, A. J. Zattera, *Structural Characteristics and Thermal Properties of Native Cellulose, in Cellulose: Fundamental Aspects* (Ed.: T. van de Ven, L. Godbout), InTech, **2013**, ISBN: 978-953-51-1183-2; b) Y. Nishiyama, P. Langan, H. Chanzy, *J. Am. Chem. Soc.* **2002**, *124*, 9074–9082.

[3] a) B. Lindman, G. Karlström, L. Stigsson, *J. Mol. Liq.* **2010**, *156*, 76–81; b) M. Bergenstråhle, J. Wohlert, M. E. Himmel, J. W. Brady, *Carbohydr. Res.* **2010**, *345*, 2060–2066; c) B. Medronho, A. Romano, M. G. Miguel, L. Stigsson, B. Lindman, *Cellulose* **2012**, *19*, 581–587; d) O. Biermann, E. Hadicke, S. Koltzenburg, F. Muller-Plathe, *Angew. Chem. Int. Ed.* **2001**, *40*, 3822–3825; *Angew. Chem.* **2001**, *113*, 3938–3942; e) C. Yamane, T. Aoyagi, M. Ago, K. Sato, K. Okajima, T. Takahashi, *Polym. J.* **2006**, *38*, 819–826; f) H. Miyamoto, M. Umemura, T. Aoyagi, C. Yamane, K. Ueda, K. Takahashi, *Carbohydr. Res.* **2009**, *344*, 1085–1094.

[4] a) C. Loerbroks, R. Rinaldi, W. Thiel, *Chem. Eur. J.* **2013**, *19*, 16282–16294; b) G. A. Jeffrey, J. A. Pople, J. S. Binkley, S. Vishveshwara, *J. Am. Chem. Soc.* **1978**, *100*, 373–379; c) V. G. S. Box, *Heterocycles* **1990**, *31*, 1157–1181; d) V. G. S. Box, *Heterocycles* **1991**, *32*, 795–807; e) H. Thøgersen, R. U. Lemieux, K. Bock, B. Meyer, *Can. J. Chem.* **1982**, *60*, 44–57; f) M. K. Dowd, A. D. French, P. J. Reilly, *Carbohydr. Res.* **1992**, *233*, 15–34; g) C. J. Cramer, D. G. Truhlar, A. D. French, *Carbohydr. Res.* **1997**, *298*, 1–14; h) W. Plazinski, A. Lonardi, P. H. Hünenberger, *J. Comput. Chem.* **2016**, *37*, 354–65; i) E. J. Cocinero, P. Çarçabal, T. D. Vaden, J. P. Simons, B. G. Davis, *Nature* **2011**, *469*, 76–79.

[5] T. Heinze, A. Koschella, T. Liebert, V. Harabagiu, S. Coseri, in *The European Polysaccharide Network of Excellence (EPNOE)-Cellulose: Chemistry of Cellulose Derivatization* (Ed.: P. Navard), Springer, Wien, **2012**, pp. 283–323.

[6] a) K. Shintate, M. Kitaoka, Y. K. Kim, K.; Hayashi, *Carbohydr. Res.* **2003**, *338*, 1981–1990; Hayashi, *Carbohydr. Res.* **2003**, *338*, 1981–1990; b) H. Nakai, M. Abou Hachem, B. O. Petersen, Y. Westphal, K. Mannerstedt, M. J. Baumann, A. Dilokpimol, H. A. Schols, J. O. Duus, B. Svensson, *Biochimie* **2010**, *92*, 1818–1826.

[7] a) M. D. Kaufman Rechulski, M. Käldström, U. Richter, F. Schüth, R. Rinaldi, *Ind. Eng. Chem. Res.* **2015**, *54*, 4581 – 4592; b) S. M. Hick, C. Griebel, D. T. Restrepo, J. H. Truitt, E. J. Buker, C. Bylda, R. G. Blair, *Green Chem.* **2010**, *12*, 468 – 474; c) R. G. Blair, K. Chagoya, S. Biltek, S. Jackson, A. Sinclair, A. Taraboletti, D. Restrepo, *Faraday Discuss.* **2014**, *170*, 223 – 233; d) N. Meine, R. Rinaldi, F. Schüth, *ChemSusChem* **2012**, *5*, 1449 – 1454; e) Q. Zhang, F. Jérôme, *ChemSusChem* **2013**, *6*, 2042 – 2044; f) F. Jérôme, K. De Oliveira Vigier, G. Chatel, *Green Chem.* **2016**, *18*, 3903 – 3913.

[8] a) M. Benoit, A. Rodrigues, Q. Zhang, E. Fourré, K. De Oliveira Vigier, J.-M. Tatibouët, F. Jérôme, *Angew. Chem. Int. Ed.* **2011**, *50*, 8964 – 8967; *Angew. Chem.* **2011**, *123*, 9126 – 9129; b) M. Benoit, A. Rodrigues, K. De Oliveira Vigier, E. Fourré, J. Barrault, J.-M. Tatibouët, F. Jérôme, *Green Chem.* **2012**, *14*, 2212 – 2215.

[9] Y. Sasai, Y. Yamauchi, S.-I. Kondo, M. Kuzuya, *Chem. Pharm. Bull.* **2004**, *52*, 339 – 344.

[10] a) A. Zille, F. R. Oliveira, A. P. Souto, *Plasma Processes Polym.* **2015**, *12*, 98 – 131; b) K. Johansson, in *Plasma Technologies for Textiles* (Ed.: R. Shishoo), **2007**, Woodhead, Cambridge; c) E. Bozaki, K. Sever, M. Sarikanat, Y. Seki, A. Demir, E. Ozdogan, *Composites Part B* **2013**, *45*, 565 – 572; d) E. Nithya, R. Radhai, R. Rajendran, S. Shalini, V. Rajendran, S. Jayakumar, *Carbohydr. Polym.* **2011**, *83*, 1652 – 1658; e) K. Kolářová, V. Vosmanská, S. Rimpelová, V. Švorčík, *Cellulose* **2013**, *20*, 953 – 961.

[11] a) T. L. Ward, H. Z. Jung, O. Hinojosa, R. R. Benerito, *J. Appl. Polym. Sci.* **1979**, *23*, 1987 – 2003; b) M. Kuzuya, K. Morisaki, J. Niwa, Y. Yamauchi, K. Xu, *J. Phys. Chem.* **1994**, *98*, 11301 – 11307.

[12] J. H. Wiley, R. H. Atalla, *Carbohydr. Res.* **1987**, *160*, 113 – 129.

[13] a) D. L. Dalluge, T. Daugaard, P. Johnston, N. Kuzhiyil, M. M. Wrighta, R. C. Brown, *Green Chem.* **2014**, *16*, 4144 – 4155; b) N. Kuzhiyil, D. Dalluge, X. Bai, K. H. Kim, R. C. Brown, *ChemSusChem* **2012**, *5*, 2228 – 2236.

[14] I. Ciucanu, C. E. Costello, *J. Am. Chem. Soc.* **2003**, *125*, 16213 – 16219.

[15] J. S. Kim, B. L. Reuhs, F. Michon, R. E. Kaiser, G. Arumugham, *Carbohydr. Res.* **2006**, *341*, 1061 – 1064.

[16] G. Sassaki, P. Gorin, L. Souza, P. Czelusniak, M. Lacomini, *Carbohydr. Res.* **2005**, *340*, 731 – 739.

[17] J. Delaux, M. Nigen, E. Fourré, J.-M. Tatibouët, A. Barakat, L. Atencio, J. M. García Fernández, K. De Oliveira Vigier, F. Jérôme, *Green Chem.* **2016**, *18*, 3013 – 3019.

Received: July 6, 2016
Published online on September 30, 2016